The thermodynamic H^+/ATP ratios of the H^+-ATPsynthases from chloroplasts and *Escherichia coli*

Stefan Steigmiller*, Paola Turina†, and Peter Gräber*‡

*Institut für Physikalische Chemie, Universität Freiburg, Albertstrasse 23a, D-79104 Freiburg, Germany; and †Department of Biology, Laboratory of Biochemistry and Biophysics, University of Bologna, Via Irnerio 42, I-40126 Bologna, Italy

Edited by Pierre A. Joliot, Institut de Biologie Physico-Chimique, Paris, France, and approved January 15, 2008 (received for review September 4, 2007)

The H^+/ATP ratio is an important parameter for the energy balance of all cells and for the coupling mechanism between proton transport and ATP synthesis. A straightforward interpretation of rotational catalysis predicts that the H^+/ATP coincides with the ratio of the c-subunits to β-subunits, implying that, for the chloroplast and *Escherichia coli* ATPsynthases, numbers of 4.7 and 3.3 are expected. Here, the energetics described by the chemiosmotic theory was used to determine the H^+/ATP ratio for the two enzymes. The isolated complexes were reconstituted into liposomes, and parallel measurements were performed under identical conditions. The internal phase of the liposomes was equilibrated with the acidic medium during reconstitution, allowing to measure the internal pH with a glass electrode. An acid–base transition was carried out and the initial rates of ATP synthesis or ATP hydrolysis were measured with luciferin/luciferase as a function of ΔpH at constant $Q = [ATP]/([ADP][P_i])$. From the shift of the equilibrium ΔpH as a function of Q the standard Gibbs free energy for phosphorylation, $\Delta G_p^{0\prime}$; and the H^+/ATP ratio were determined. It resulted $\Delta G_p^{0\prime} = 38 \pm 3$ kJ·mol^{-1} and $H^+/ATP = 4.0 \pm 0.2$ for the chloroplast and $H^+/ATP = 4.0 \pm 0.3$ for the *E. coli* enzyme, indicating that the thermodynamic H^+/ATP ratio is the same for both enzymes and that it is different from the subunit stoichiometric ratio.

ATPase | F0F1 | proteoliposomes | chemiosmotic theory

Membrane-bound H^+-ATPsynthases play a central role in the energy metabolism of all cells: They catalyze the synthesis of ATP from ADP and inorganic phosphate (P_i) in bacteria, chloroplasts, and mitochondria (1–4). In these organelles, electron-transport generates a transmembrane electrochemical potential difference of protons, $\Delta\tilde{\mu}_{H^+}$, and the H^+-ATPsynthase couples the $\Delta\tilde{\mu}_{H^+}$-driven proton efflux with ATP synthesis (5, 6).

All H^+-ATPsynthases have a similar structure: the hydrophilic F_1 part with subunits $\alpha_3\beta_3\gamma\delta\varepsilon$ contains the nucleotide and P_i binding sites, and the membrane integrated F_0 part, with subunits ab_2c_{10} in *Escherichia coli* (I, II, III_{14}, and IV in chloroplasts), contains the proton binding sites. The kinetics of the enzyme was described by the binding change theory, in which the cooperativity of the three catalytic binding sites is accomplished by γ-subunit rotation (7). The high-resolution x-ray structure of F_1 corroborated this theory showing that the centrally located γ-subunit interacts differently with the three β-subunits and that the catalytic site on each β-subunit has a different conformation (8). Rotation of the γ-subunit was observed with different experimental techniques (9–11).

Current models of the coupling of proton translocation to ATP synthesis assume that proton flow through the F_0 part drives a rotation of the ring of c-subunits against the a- and b-stator subunits; the connection of the c-subunits to the γ- and ε-subunits leads to rotation of the latter within the $\alpha_3\beta_3$ barrel, which brings about the conformational changes at the catalytic sites required for ATP synthesis. To accomplish rotation of the c-ring, protons are assumed to enter the F_0 part through an access channel on one side of the membrane, bind to the essential glutamate (or aspartate) on subunit c, and leave it through an asymmetrically placed exit channel on the other side (12–15). Cross-linking data (16–18), single molecule visualization (19–21), polarization data (22), and FRET measurements (23) indicate that the ring of c-subunits in F_0 rotates together with the γ- and ε-subunit in F_1.

This mechanism appears to directly predict the H^+/ATP ratio: It should be equal to the number of c-subunits, divided by the number of β-subunits. Whereas all known F_0F_1-ATPsynthases contain three β-subunits, the number of c-subunits seems to be species-dependent. It has been reported to be 10 in mitochondria (24), 14 in chloroplasts (25), 10 in *E. coli* (26) and PS3 (27), 11 in the Na^+-ATP synthase from *Ilyobacter tartaricus* (28), and 13 in Bacillus sp. strain TA2A1 (29). The unexpected β–c stoichiometric ratio mismatch (pointing to a nonintegral value of the H^+/ATP ratio) and species specificity have stimulated anew much interest in this number (see, e.g., ref. 30).

The H^+/ATP ratio is important not only for understanding the coupling mechanism of the enzyme, but also for the energy balance of cells. Values of H^+/ATP between 2 and 4 have been reported and also variable ones (reviewed in ref. 31). The most recent data give $H^+/ATP = 4$ for the chloroplast enzyme (32–34), whereas $H^+/ATP = 3$ was reported for the mitochondrial enzyme (reviewed in ref. 35). Few data on the H^+/ATP ratio of the *E. coli* enzyme are found in the literature (31), pointing to values between 2 and 3.6.

Results

To determine the H^+/ATP ratio in the absence of other interfering reactions taking place in energy transducing membranes, we set up a minimal chemiosmotic system containing only the H^+-ATPsynthase and a lipid membrane. Liposomes from phosphatidylcholine/phosphatidic acid were prepared, and either CF_0F_1 or EF_0F_1 was reconstituted into these liposomes with a stoichiometric ratio of $\approx$1 CF_0F_1 or 3 EF_0F_1 per liposome [see supporting information (SI) Fig. 4]. These liposomes catalyze high rates of ATP synthesis (36, 37) when subjected to an acid-base transition (38).

The chemiosmotic theory describes the thermodynamics of the coupling between proton transport and ATP synthesis. For the chemical reaction,

Author contributions: S.S., P.T., and P.G. designed research; S.S. and P.T. performed research; S.S., P.T., and P.G. analyzed data; and S.S., P.T., and P.G. wrote the paper.

The authors declare no conflict of interest.

This article is a PNAS Direct Submission.

Freely available online through the PNAS open access option.

‡To whom correspondence should be addressed. E-mail: peter.graeber@physchem.uni-freiburg.de.

This article contains supporting information online at www.pnas.org/cgi/content/full/0708356105/DC1.

$$ADP + P_i \rightleftharpoons ATP + H_2O \quad [1]$$

the Gibbs free energy of ATP synthesis is given by

$$\Delta G'_p = \Delta G^{0\prime}_p + RT\ln\frac{[ATP]c^0}{[ADP][P_i]} = \Delta G^{0\prime}_p + 2.3RT\lg Q, \quad [2]$$

where $\Delta G^{0\prime}_p$ is the Gibbs free energy in the biochemical standard state, Q is the stoichiometric product, and c^0 is the standard concentration (equal to 1 M).

Proton transport from the internal to the external phase is described by the following equation:

$$nH^+_{in} \rightleftharpoons nH^+_{out} \quad [3]$$

with $n = H^+/ATP$. Using the definitions $\Delta pH = pH_{out} - pH_{in}$ and $\Delta\varphi = \varphi_{in} - \varphi_{out}$, the transmembrane electrochemical potential difference of protons (Gibbs free energy of proton transport) is given by

$$\begin{aligned}\Delta\tilde{\mu}_{H^+} &= \tilde{\mu}_{H^+}(in) - \tilde{\mu}_{H^+}(out)\\ &= RT\ln[H^+_{in}] - RT\ln[H^+_{out}] + F\varphi_{in} - F\varphi_{out}\\ &= 2.3RT(pH_{out} - pH_{in}) + F(\varphi_{in} - \varphi_{out})\\ &= 2.3RT\Delta pH + F\Delta\varphi \quad [4]\end{aligned}$$

The Gibbs free energy of the coupled reaction is the sum of Eqs. **2** and **4**, i.e.,

$$\begin{aligned}\Delta G' &= \Delta G'_p - n\Delta\tilde{\mu}_{H^+}\\ &= \Delta G^{0\prime}_p + 2.3RT\lg Q - n2.3RT\Delta pH - F\Delta\varphi. \quad [5]\end{aligned}$$

At the point of equilibrium of the coupled reaction ($\Delta G' = 0$) and with $\Delta\varphi = 0$, we obtain from Eq. **5**:

$$+ 2.3RT\lg Q = - \Delta G^{0\prime}_p + n2.3RT\Delta pH(eq). \quad [6]$$

With experimentally determined Q and $\Delta pH(eq)$, the unknown parameters in Eq. **6** are the H^+/ATP ratio, n, and the phosphorylation standard free energy, $-\Delta G^{0\prime}_p$.

The different parameters in Eqs. **5** and **6** were determined as follows.

- $\Delta\varphi$. An acid-to-base transition gives rise to a transmembrane ionic imbalance, which automatically generates a diffusion potential, $\Delta\varphi$. We have short-circuited it by using the same high K^+ concentration (50 mM) on both sides of the membrane in the presence of 10 μM valinomycin. Under these conditions, the contribution of all other ions to the Goldmann diffusion potential was negligible, and $\Delta\varphi = 0$.
- ΔpH. For reconstitution of the enzyme, the liposome membrane was permeabilized by addition of detergent. We assume that, during this process (2 h), a full equilibration of all ion concentrations between the internal and external phases has taken place, so that the composition of the internal phase is known. Correspondingly, the pH_{in} value was taken to be identical to the pH of the reconstitution buffer, which was measured with a glass electrode after the reconstitution. The pH_{out} value resulted from the mixing of the acidic reconstitution buffer containing the proteoliposomes with the basic medium and was measured with the same glass electrode. The error of the absolute pH was considered to result from the limited precision of the calibration buffers, with a standard deviation of ± 0.02 pH units. We have varied the pH_{in} values at constant pH_{out}, i.e., the error associated with ΔpH was $\pm$ 0.03 pH units.
- $\Delta pH(eq)$. For each given Q value, the rates of ATP synthesis and ATP hydrolysis were measured as a function of ΔpH, and the $\Delta pH(eq)$ was interpolated as the value at which the rate was zero.
- Q. The stoichiometric product Q was established by setting the ADP, ATP, and P_i concentrations to the desired values. Because we measured initial rates of ATP synthesis and ATP hydrolysis (slope at $t = 0$), substrate and product concentrations remained at their preestablished values. Therefore, the error in $\lg Q$ was very small and was neglected in our analysis.

To measure the initial rates of ATP synthesis and ATP hydrolysis, an ATP-monitoring luciferin/luciferase mixture was added to the basic medium in a luminometer cuvette. Additionally, the baseline of luminescence was recorded indicating the ATP concentration in the medium at the preestablished Q value. At reaction time $t = 0$, the acidic buffer with proteolipomes was injected with a syringe, and the luminescence was measured for $\approx$3 min (see SI Fig. 5). The composition of the external phase resulted from the mixing of the basic medium with the acidic reconstitution buffer containing the proteoliposomes (see SI Table 1). The CF_0F_1 and EF_0F_1 concentrations in the reaction medium were 7.6 nM and 23 nM, respectively.

Some of the rate measurements with CF_0F_1 are shown in Fig. 1 *Left*. An increase of luminescence indicates ATP synthesis; a decrease indicates ATP hydrolysis. The arrows indicate the time point of injection of the proteoliposomes into the basic medium, i.e., the start of the reaction. Each panel shows the data obtained at the same constant stoichiometric product. The Q values and the corresponding concentrations of ADP, ATP, and P_i are collected in SI Table 2. The different curves within each panel refer to different ΔpH values, and the slope of each curve at $t = 0$ gives the initial rate in units of ATP per enzyme per second. In each panel, the initial rate switches from ATP synthesis at the highest ΔpH to ATP hydrolysis at the lowest ΔpH. No change in ATP concentration was observed when the ΔpH was dissipated by 10 μM nigericin, indicating both the absence of adenylate kinase activity and the absence of ATP hydrolysis when the enzyme was not activated by a ΔpH.

Similar measurements were carried out with EF_0F_1, using the same method. For both enzymes, reconstitutions were carried out in parallel, using the same buffers, mixing ratios, pH electrode, etc. The only difference was that the EF_0F_1 proteoliposomes contained a 3-fold higher average number of ATPsynthase molecules per liposome. Despite this higher enzyme concentration, the signal-to-noise ratio in the EF_0F_1 traces was significantly lower. Lower absolute rates in EF_0F_1 were expected, because the maximal ATP synthesis turnover of EF_0F_1 was 80 s^{-1} compared with 280 s^{-1} for CF_0F_1. Moreover, in the present measurements, the $\Delta\varphi$ was clamped to 0 and the EF_0F_1 turnover decreases much stronger with $\Delta\varphi$ than that of CF_0F_1 (37).

Fig. 1 *Right* shows rate measurements with EF_0F_1 from Q = 12 to Q = 152. For each stoichiometric product, ATP synthesis is observed at the highest ΔpH and ATP hydrolysis at the lowest. In all ATP synthesis traces, the initial rate decreases and switches to ATP hydrolysis after 5–20 s. This reflects the decrease of the initial ΔpH due to proton efflux. The data in the presence of 10 μM nigericin indicate the absence of ATP hydrolysis and adenylate kinase activities; at Q = 152, a constant ATP concentration is initially observed, followed by a slow decrease of ATP, i.e., the enzyme is initially inactive and is activated by binding and hydrolysis of ATP.

For both enzymes, the initial rates and their errors were evaluated by monoexponential fitting of the first part of the traces (see details in SI Fig. 6) and were plotted versus ΔpH (see Fig. 2). At the thermodynamic equilibrium, catalysis switches from ATP synthesis to ATP hydrolysis, and this point, $\Delta pH(eq)$, was determined by interpolation.

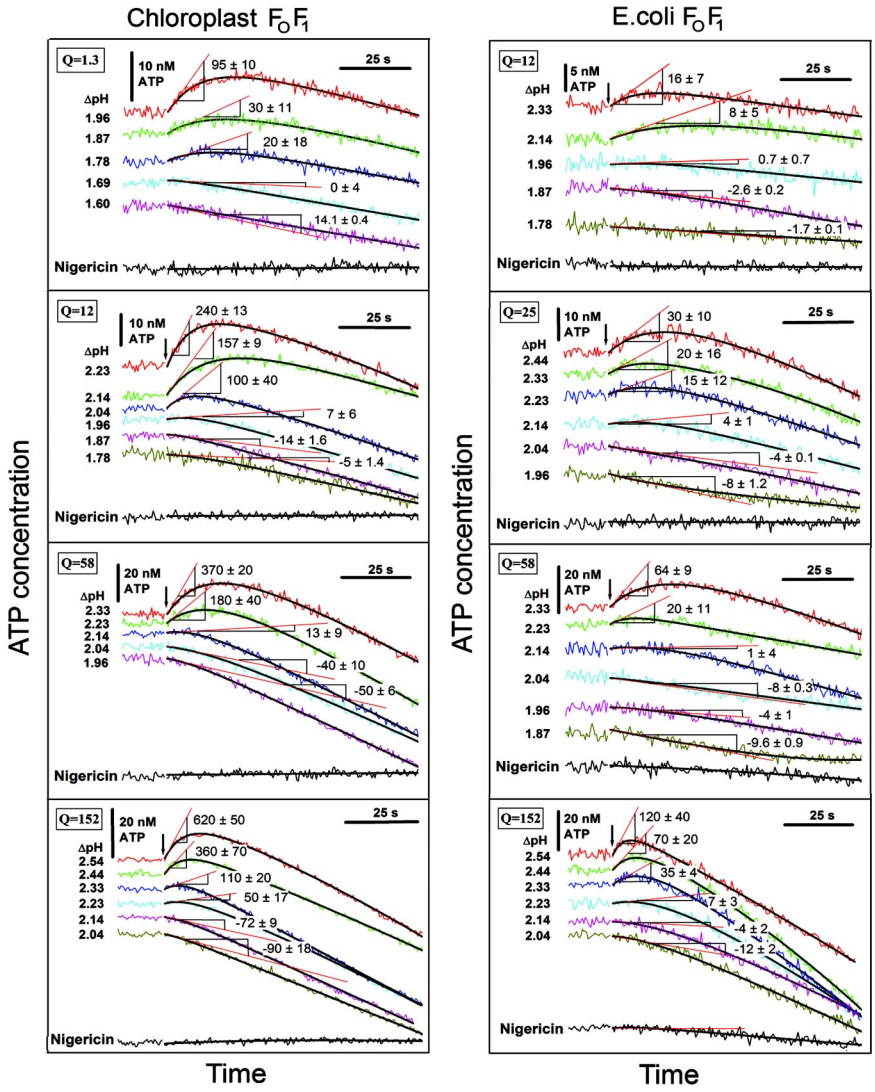

Fig. 1. ATP synthesis and ATP hydrolysis after generation of a transmembrane ΔpH. The basic medium (900 μl) with the preestablished *Q* value and with luciferin/luciferase was placed into a cuvette in the luminometer, and the baseline was registered. The acid-base transitions were carried out by injection of 100 μl of proteoliposomes, incubated in the acidic reconstitution medium at different pH_{in}. The final pH_{out} was 8.47 ± 0.02, and the ΔpH values are given next to each trace. The addition gives rise to an immediate jump of the baseline. For clarity, the baseline was shifted back to the original luminescence level. The luminescence increase indicates ATP synthesis, the decrease indicates ATP hydrolysis. The different panels refer to different stoichiometric ratios *Q* as indicated. The luminescence was calibrated by addition of standard ATP. The solid lines show a biexponential fit of the complete time trace. The initial rates and their errors are given in units of 10^{-3} s^{-1}; they were calculated from the monoexponential fit of the first part of the traces, as detailed in SI Fig. 6. (*Left*) CF_0F_1 proteoliposomes. The final CF_0F_1 concentration was 7.6 nM. (*Right*) EF_0F_1 proteoliposomes. The final EF_0F_1 concentration was 23 nM.

The activity of CF_0F_1 is regulated by a disulfide bridge in the γ-subunit and by ΔpH (39–42). When CF_0F_1 is in its reduced state—achieved in this work by incubation with DTT—the rate of coupled ATP hydrolysis is controlled by two opposing effects. With decreasing ΔpH, the back pressure of protons is decreased; thus, the hydrolysis rate should increase, but the fraction of active enzyme also decreases, thus decreasing this rate. Both effects can be seen in Fig. 1 *Left*. When the ΔpH is collapsed by nigericin, i.e., the enzyme is not activated, no hydrolysis is detected. An increase of the hydrolysis rate with increasing reaction time, i.e., with decreasing ΔpH, can also be observed (see, e.g., trace at $Q = 58$, ΔpH = 1.96).

Only active enzymes catalyze proton transport coupled ATP synthesis/hydrolysis. Whereas the rates depend on the number of active enzymes, the position of the equilibrium described by Eq. **6** does not. The rates were measured in this work close to equilibrium, so that the activation should not influence the interpolated ΔpH(eq). Nevertheless, we corrected for the effect of activation as described in ref. 34 by taking into account the sigmoidal ΔpH dependency measured in thylakoid membranes (40) (SI Fig. 7 shows the corrected rates as a function of ΔpH). The interpolated ΔpH(eq) values were, within error limits, the same for the original and the corrected data (see SI Table 1).

Regulatory phenomena dependent on $\Delta\tilde{\mu}_{H^+}$ have been shown in EF_0F_1 as well (43), although a quantitative ΔpH dependency is not available. The EF_0F_1 traces of Fig. 1 *Right* are consistent with a kinetic control exerted by ΔpH: similar to CF_0F_1, no hydrolysis is detected when the ΔpH is collapsed by nigericin, and an increase of the hydrolysis rate with increasing reaction time (i.e., with decreasing ΔpH) can be observed in several traces.

The ΔpH(eq) determined in Fig. 2 for both enzymes and the corresponding *Q* values were then plotted as 2.3RTlg*Q* versus 2.3RTΔpH(eq) in Fig. 3 *Upper*. According to Eq. **6**, such a plot should yield a straight line with slope *n* (the thermodynamic

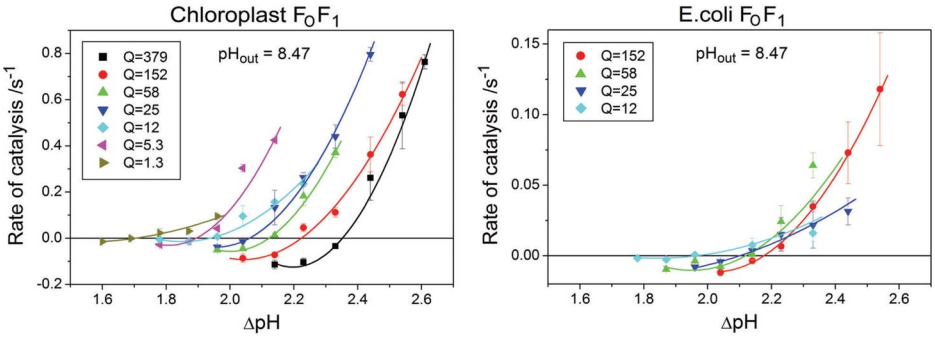

Fig. 2. Rate of ATP synthesis and hydrolysis as a function of the transmembrane ΔpH. The initial rates and their errors obtained from Fig. 1, and additional measurements, were plotted as a function of ΔpH. Some error bars are not visible, because they are smaller than the size of the symbols. Each curve represents catalysis rates measured at a constant stoichiometric product, *Q*. The data were fitted, using their errors as weight, by a function that was the product of a linear function (describing the rate-force relation near equilibrium) and of a sigmoidal function (describing the ΔpH dependence of activation). The fitting functions were used to interpolate the point at which the rate is zero [ΔpH(eq)]. (*Left*) CF_0F_1 proteoliposomes. (*Right*) EF_0F_1 proteoliposomes.

H^+/ATP ratio) and axis intercept $-\Delta G_p^{0\prime}$. The fitting by linear regression of the CF_0F_1 data (Fig. 3 *Upper Left*) gave values of $n = 4.0 \pm 0.2$ and $\Delta G_p^{0\prime} = (38 \pm 3)$ kJ·mol^{-1}. The fitting by linear regression of the corresponding EF_0F_1 data (Fig. 3, *Upper Right*) gave values of n and $-\Delta G_p^{0\prime}$, which were loaded with a much higher uncertainty, mainly due to the limited range of Q values and ΔpH(eq) obtained for EF_0F_1. Therefore, the CF_0F_1 dataset was used as a reference, and the $-\Delta G_p^{0\prime}$ resulting from their fit was included in the EF_0F_1 dataset. The linear regression of these data yielded a value of $n = 4.0 \pm 0.3$, i.e., very similar to the value obtained for CF_0F_1. The dashed line has been drawn by imposing $n = 3.3$ (with $\Delta G_p^{0\prime} = 38$ kJ·mol^{-1}), and the dotted lines indicate that the expected ΔpH(eq) values in this case should have been ≈0.5 ΔpH units higher.

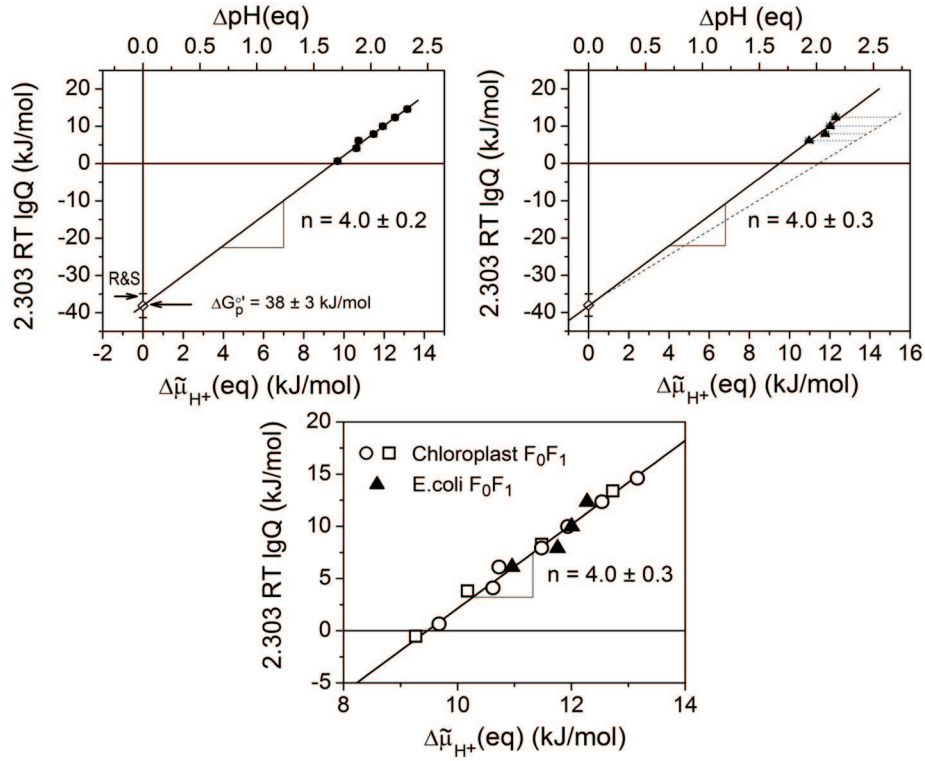

Fig. 3. Determination of the thermodynamic H^+/ATP ratio. ΔpH(eq) was plotted versus the stoichiometric product *Q* according to Eq. **6** (data from Fig. 2). (*Upper Left*) CF_0F_1 data (from Fig. 2 *Left*). The error associated with ΔpH(eq) has been taken to coincide with the error estimated for ΔpH determination by the pH electrode (±0.03). The data were fitted by a straight line, using their errors as weight. The slope of the linear regression gives the H^+/ATP ratio. The *y* intercept gives the standard Gibbs free energy $-\Delta G_p^{0\prime}$ at $pH_{out} = 8.47$. The arrow marked as R&S indicates the value of $-\Delta G_p^{0\prime}$ published in ref. 43. (*Upper Right*) EF_0F_1 data (from Fig. 2 *Right*). The $-\Delta G_p^{0\prime}$ value (diamond) is the best-fitting parameter out of the CF_0F_1 data (*Left*) and has been included in the linear regression of the EF_0F_1 data. The data were fitted by a straight line, using their errors as weight. The slope of the linear regression gives the H^+/ATP ratio. To account for the error on the *y* axis of the $\Delta G_p^{0\prime}$ value, two additional linear fits were calculated, using its two extreme values of 35 and 41; the resulting H^+/ATP values were 3.7 and 4.3 respectively, whose difference from 4.0, being higher than the error resulting from each linear regression, has been taken as the error in the determination of this parameter. (*Lower*) The CF_0F_1 (circles) and EF_0F_1 (triangles) data from *Upper* are plotted together for better comparison; the squares are CF_0F_1 data from ref. 34, in which the $\Delta\varphi$ component has been converted in ΔpH units (15 mV, corresponding to 0.26 ΔpH units). The straight line is the regression line of *Upper Left*.

In Fig. 3 *Lower*, the CF_0F_1 (circles) and EF_0F_1 (triangles) data are plotted together for better comparison. Also plotted are the previously obtained CF_0F_1 data from (34) (squares); the latter data had been measured in the presence of a $\Delta\varphi$ component of 15 mV.

It is interesting that the data presented in Fig. 2 can also be analyzed in a reciprocal manner by plotting the rates obtained at constant ΔpH versus RTln$Q$ and determining RTln$Q$(eq) by interpolation (SI Fig. 8). When the interpolated RTln$Q$(eq) data were plotted versus 2.3RTΔpH, a straight line was obtained with a slope of $n = 4.1 \pm 0.2$ and $\Delta G_p^{0\prime} = 39 \pm 3$ for CF_0F_1 and a slope of $n = 4.0 \pm 0.3$ for EF_0F_1 (SI Fig. 9).

Discussion

The aim of this work was to determine the H^+/ATP ratio from two H^+-ATPsynthases, which show differences in the c/β stoichiometric ratio, in particular EF_0F_1 and CF_0F_1, for which the c/β stoichiometric ratios have been reported as 3.3 and 4.7, respectively. The thermodynamic parameters of proton transport coupled ATP synthesis/hydrolysis were measured under identical conditions for CF_0F_1 and EF_0F_1 and the H^+/ATP ratio for both enzymes was obtained from the change of the equilibrium ΔpH with ln$Q$.

These identical experimental conditions allowed us to use, for evaluating the EF_0F_1 data, the $\Delta G_p^{0\prime}$ value, which was obtained with higher precision from the CF_0F_1 data, thereby lowering the error limits in the H^+/ATP determination for EF_0F_1. In fact, because of the lower rate of EF_0F_1, these measurements could not be extended to the wide range of Q values required to determine with high precision both $\Delta G_p^{0\prime}$ and H^+/ATP. The analysis of the CF_0F_1 data resulted in $\Delta G_p^{0\prime} = 38 \pm 3$ kJ·mol^{-1} and H^+/ATP $= 4.0 \pm 0.2$. Using this $\Delta G_p^{0\prime}$ value, the EF_0F_1 data gave H^+/ATP $= 4.0 \pm 0.3$. It is evident that, similarly to CF_0F_1, the measured thermodynamic H^+/ATP ratio in EF_0F_1 is not consistent with the reported subunit stoichiometric ratio (26).

The H^+/ATP ratio of 4 obtained for CF_0F_1 is in accordance with earlier results (32–34), and $\Delta G_p^{0\prime}$ is in accordance with data in ref. 44. Values of 2–3.6 have been reported for H^+/ATP in EF_0F_1; however, these measurements included use of indirect probes (45) and assumptions for estimating $\Delta\tilde{\mu}_{H+}$ and $\Delta G_p^{0\prime}$ in whole cells (46, 47).

The reason for the surprising difference found here between the thermodynamic H^+/ATP and the c/β stoichiometric ratio is not known yet. The thermodynamic H^+/ATP ratio reflects the minimal number of H^+ necessary for ATP synthesis (or hydrolysis) of one ATP at equilibrium. At high rates of ATP synthesis far from equilibrium, it is conceivable that additional protons have to be translocated through the enzyme for each synthesized ATP, e.g., slip protons, leading to what can be called a "kinetic" H^+/ATP ratio. It might be that the c/β stoichiometric ratio is optimized for such high rates, which would explain the mismatch between that ratio and the thermodynamic H^+/ATP ratio. However, earlier proton flux measurements carried out far from equilibrium with thylakoid membranes also gave H^+/ATP $= 4$ (48), lending no support to this speculation.

Alternatively, these data might indicate that the number of c-subunits in the holoenzyme CF_0F_1 is different from that found in the isolated ring of subunit III. As to the *E. coli* enzyme, it has been suggested that the number of c-subunits in this organism might change in response to the prevailing metabolic conditions (31), which would imply that the issue of the c-subunit number is not definitively settled in this organism either. The discrepancy presently found between the thermodynamic requirements (H^+/ATP $= 4$ for both enzymes) and the subunit stoichiometric ratio (c/$\beta = 3.3$ for EF_0F_1 and c/$\beta = 4.7$ for CF_0F_1) raises interesting questions for future research.

Materials and Methods

CF_0F_1 from spinach (*Spinacia oleracea*) was isolated as described in ref. 34. CF_0F_1 was obtained in a buffer containing 1.25 M sucrose, 30 mM NaH_2PO_4/NaOH (pH 7.2), 2 mM $MgCl_2$, 0.5 mM Na_2EDTA, and 4 mM dodecyl maltoside, with a protein concentration of 4.2 mg/ml, and stored at −80°C. EF_0F_1 from pBWU13 *E. coli* strain DK8 (Δunc) was isolated as described in refs. 49 and 50. The EF_0F_1 complex was obtained in a buffer containing 0.9 M sucrose; 10 mM Mes; and 10 mM Tricine/NaOH (pH 7.0), 0.5 mM $MgCl_2$, 5 mM thioglycerol, and 10 g/liter octyl glucoside, with a protein concentration of 2.2 mg/ml, and stored in liquid nitrogen.

Liposomes from phosphatidylcholine and phosphatidic acid were prepared by dialysis and stored at −80°C (37). CF_0F_1 or EF_0F_1 was reconstituted into these preformed liposomes with 0.8% Triton X-100 and Biobeads (stored in 50 mM KCl), using buffers at 12 different pH values. These acidic buffers contained 25 mM Mops/NaOH, 25 mM Mes/NaOH, 50 mM KCl, 4.4 mM $MgCl_2$ (3.15 mM + 1.25 mM from the dialysis buffer), and 2.5 mM NaH_2PO_4 plus 5 mM Tricine, 0.1 mM EDTA, and 0.1 mM DTT from the dialysis buffer. Because of Triton X-100 treatment during reconstitution, all ion concentrations can be considered to have equilibrated between the bulk phase and the internal proteoliposome phase. The pH was measured with a glass electrode after reconstitution and is referred to as pH_{in}. The final enzyme concentrations were 80 nM for CF_0F_1 and 240 nM for EF_0F_1.

The ATP concentration was measured with luciferin/luciferase (34). All suspensions and solutions were equilibrated at room temperature (23°C). Valinomycin was added to proteoliposomes to a final concentration of 10 μM. A luminometer cuvette was filled with 20 μl of luciferin/luciferase kit; 349 μl of a solution containing 100 mM KCl and 9 mM $MgCl_2$; 1 μl of a solution containing 1 M DTT and 50 mM KCl; 200 μl of a solution at pH 8.60 (containing 0.5 M Tricine, 5 mM NaH_2PO_4, 4.5 mM $MgCl_2$, 50 mM KOH, and 330 mM NaOH); and 330 μl of a solution containing different concentrations of ADP and ATP (final volume 900 μl). The reaction was started by injection of 100 μl of proteoliposomes into the cuvette placed in the luminometer. The pH value measured after this mixing was the pH of the external phase during the ΔpH transition (pH_{out}). The resulting ion concentrations of the internal and external phases and the nucleotide concentrations are summarized in SI Tables 2 and 3. The final ATP and ADP concentrations were 25 ÷ 800 nM and 1.7 ÷ 16 μM, and the final P_i concentration was 1.25 mM. The luminescence signal was calibrated by three additions of 10 μl of an ATP standard (10^{-5} M) to each cuvette. The luminescence data were sampled in 55-ms intervals. In the graphical representation of the data in Fig. 1, ten 55-ms time intervals have been averaged to reduce the noise. To calculate the initial rates and their errors, the initial phases of the signals at the original time resolution were fitted with either a monoexponential or a linear function (using the software package Origin). SI Fig. 6 shows the luminescence time traces at the original time resolution, the fitted functions, and the residuals for one Q value ($Q = 152$).

Measurements of the rate of ATP synthesis under standard conditions ($pH_{in} = 4.8$, $pH_{out} = 8.5$, $[K^+_{in}] = 50$ mM, $[K^+_{out}] = 180$ mM) were carried out as described in ref. 37. Concentrations of ATP and ADP were measured as described in ref. 34. The ATP content in ADP solutions was 0.16%.

ACKNOWLEDGMENTS. We thank Jan Petersen and Giovanni Venturoli for discussions and for their generous help. This work was supported by the Programmi di ricerca di Rilevante Interesse Nazionale Project 2005052128_004 from the Italian Ministry for Education of University and Research (to P.T.). S.S. was a fellow of the Studienstiftung des Deutschen Volkes.

1. Yoshida M, Muneyuki E, Hisabori T (2001) ATP synthase—A marvellous rotary engine of the cell. *Nat Rev Mol Cell Biol* 2:669–677.
2. Senior AE, Nadanaciva S, Weber J (2002) The molecular mechanism of ATP synthesis by F_1F_0-ATP synthase. *Biochim Biophys Acta* 1553:188–211.
3. Kinosita K, Jr., Adachi K, Itoh H (2004) Rotation of F_1-ATPase: How an ATP-driven molecular machine may work. *Annu Rev Biophys Biomol Struct* 33:245–268.
4. Wilkens S (2005) Rotary molecular motors. *Advan Protein Chem* 71:345–382.
5. Mitchell P (1961) Coupling of phosphorylation to electron and hydrogen transfer by chemi-osmotic type of mechanism. *Nature* 191:144–152.
6. Mitchell P (1966) Chemiosmotic coupling in oxidative and photosynthetic phosphorylation. *Biol Rev* 41:445–502.
7. Boyer PD (1993) The binding change mechanism for ATP synthase—Some probabilities and possibilities. *Biochim Biophys Acta* 1140:215–250.
8. Abrahams JP, Leslie AG, Lutter R, Walker JE (1994) Structure at 2.8 Å resolution of F_1-ATPase from bovine heart mitochondria. *Nature* 370:621–628.
9. Duncan TM, Bulygin VV, Zhou Y, Hutcheon ML, Cross RL (1995) Rotation of subunits during catalysis by *Escherichia coli* F1-ATPase. *Proc Natl Acad Sci USA* 92:10964–10968.

10. Sabbert D, Engelbrecht S, Junge W (1996) Intersubunit rotation in active F-ATPase. *Nature* 381:623–625.
11. Noji H, Yasuda R, Yoshida M, Kinosita K, Jr (1997) Direct observation of the rotation of F_1-ATPase. *Nature* 386:299–302.
12. Junge W, Lill H, Engelbrecht S (1997) ATP synthase: An electrochemical transducer with rotatory mechanics. *Trends Biochem Sci* 22:420–423.
13. Rastogi VK, Girvin ME (1999) Structural changes linked to proton translocation by subunit c of the ATP synthase. *Nature* 402:263–268.
14. Dimroth P, Wang H, Grabe M, Oster G (1999) Energy transduction in the sodium F-ATPase of *Propionigenium modestum*. *Proc Natl Acad Sci USA* 96:4924–4929.
15. Fillingame RH, Angevine CM, Dmitriev OY (2003) Mechanics of coupling proton movements to c-ring rotation in ATP synthase. *FEBS Lett* 555:29–34.
16. Zhou Y, Duncan TM, Cross RL (1997) Subunit rotation in *Escherichia coli* FoF1-ATP synthase during oxidative phosphorylation. *Proc Natl Acad Sci USA* 94:10583–10587.
17. Jones PC, Hermolin J, Jiang W, Fillingame RH (2000) Insights into the rotary catalytic mechanism of F_0F_1 ATP synthase from the cross-linking of subunits b and c in the *Escherichia coli* enzyme. *J Biol Chem* 275:31340–31346.
18. Capaldi RA, Aggeler R (2002) Mechanism of the F_1F_0-type ATP synthase, a biological rotary motor. *Trends Biochem Sci* 27:154–160.
19. Pänke O, Gumbiowski K, Junge W, Engelbrecht S (2000) F-ATPase: Specific observation of the rotating c subunit oligomer of EF_0EF_1. *FEBS Lett* 472:34–38.
20. Nishio K, Iwamoto-Kihara A, Yamamoto A, Wada Y, Futai M (2002) Subunit rotation of ATP synthase embedded in membranes: *a* or β subunit rotation relative to the *c* subunit ring. *Proc Natl Acad Sci USA* 99:13448–13452.
21. Ueno H, Suzuki T, Kinosita K, Jr, Yoshida M (2005) ATP-driven stepwise rotation of F_0F_1-ATP synthase. *Proc Natl Acad Sci USA* 102:1333–1338.
22. Kaim G, *et al.* (2002) Coupled rotation within single F_0F_1 enzyme complexes during ATP synthesis or hydrolysis. *FEBS Lett* 525:156–163.
23. Diez M, *et al.* (2004) Proton-powered subunit rotation in single membrane-bound F_0F_1-ATP synthase. *Nat Struct Mol Biol* 11:135–141.
24. Stock D, Leslie AG, Walker JE (1999) Molecular architecture of the rotary motor in ATP synthase. *Science* 286:1700–1705.
25. Seelert H, *et al.* (2000) Structural biology. Proton-powered turbine of a plant motor. *Nature* 405:418–419.
26. Jiang W, Hermolin J, Fillingame RH (2001) The preferred stoichiometry of c subunits in the rotary motor sector of *Escherichia coli* ATP synthase is 10. *Proc Natl Acad Sci USA* 98:4966–4971.
27. Mitome N, Suzuki T, Hayashi S, Yoshida M (2004) Thermophilic ATP synthase has a decamer c-ring: Indication of noninteger 10:3 H^+/ATP ratio and permissive elastic coupling. *Proc Natl Acad Sci USA* 101:12159–12164.
28. Stahlberg H, *et al.* (2001) Bacterial Na^+-ATP synthase has an undecameric rotor. *EMBO Rep* 2:229–233.
29. Meier T, *et al.* (2007) A tridecameric c ring of the adenosine triphosphate (ATP) synthase from the thermoalkaliphilic *Bacillus* sp. strain TA2.A1 facilitates ATP synthesis at low electrochemical proton potential. *Mol Microbiol* 65:1181–1192.
30. Ferguson SJ (2000) ATP synthase: What dictated the size of a ring? *Curr Biol* 10:R804–R808.
31. Tomashek JJ, Brusilow WS (2000) Stoichiometry of energy coupling by proton-translocating ATPases: A history of variability. *J Bionenerg Biomembr* 32:493–500.
32. Van Walraven HS, Strotmann H, Schwarz O, Rumberg B (1996) The H^+/ATP coupling ratio of the ATP synthase from thiol-modulated chloroplasts and two cyanobacterial strains is four. *FEBS Lett* 379:309–313.
33. Pänke O, Rumberg B (1997) Kinetic modeling of rotary CF_0F_1-ATP synthase: Storage of elastic energy during energy transduction. *Biochim Biophys Acta* 1322:183–194.
34. Turina P, Samoray D, Gräber P (2003) H^+/ATP ratio of proton transport-coupled ATP synthesis and hydrolysis catalysed by CF_0F_1-liposomes. *EMBO J* 22:418–426.
35. Hinkle PC (2005) P/O ratios of mitochondrial oxidative phosphorylation. *Biochim Biophys Acta* 1706:1–11.
36. Possmayer F, Gräber P (1994) The pH_{in} and pH_{out} dependence of the rate of ATP synthesis catalyzed by the chloroplast H^+-ATPase, CF_0F_1 in proteoliposomes. *J Biol Chem* 269:1896–1904.
37. Fischer S, Gräber P (1999) Comparison of ΔpH- and $\Delta\varphi$-driven ATP synthesis catalyzed by the H^+-ATPases from *Escherichia coli* or chloroplasts reconstituted into liposomes. *FEBS Lett* 457:327–332.
38. Jagendorf AT, Uribe E (1966) ATP formation caused by acid-base transition of spinach chloroplasts. *Proc Natl Acad Sci USA* 55:170–177.
39. Ketcham SR, Davenport JW, Warncke K, McCarty RE (1984) Role of the gamma subunit of chloroplast Coupling Factor 1 in the light-dependent activation of phosphorylation and ATPase activity by dithiothreitol. *J Biol Chem* 259:7286–7293.
40. Junesch U, Gräber P (1987) Influence of the redox state and the activation of the chloroplast ATP synthase on proton-transport-coupled ATP synthesis/hydrolysis. *Biochim Biophys Acta* 893:275–288.
41. Kramer D, *et al.* (1990) Regulation of coupling factor in field grown sunflower: A redox model relating coupling factor activity to the activities of other thioredoxin dependent chloroplast enzymes. *Photosynth Res* 26:213–222.
42. Hisabori T, Konno H, Ichimura H, Strotmann H, Bald D (2002) Molecular devices of chloroplast F_1-ATP synthase for the regulation. *Biochim Biophys Acta* 1555:140–146.
43. Fischer S, Gräber P, Turina P (2000) Comparison of ΔpH- and $\Delta\varphi$-driven ATP synthesis catalyzed by the H^+-ATPases from *Escherichia coli* or chloroplasts reconstituted into liposomes. *J Biol Chem* 275:30157–30162.
44. Rosing J, Slater EC (1972) Nucleotide-binding properties of native and cold-treated mitochondrial ATPase. *Biochim Biophys Acta* 267:275–290.
45. Perlin DS, San Francisco MJ, Slayman CW, Rosen BP (1986) H^+/ATP stoichiometry of proton pumps from *Neurospora crassa* and *Escherichia coli*. *Arch Biochem Biophys* 248:53–61.
46. Kashket ER (1983) Stoichiometry of the H^+-ATPase of *Escherichia coli* cells during anaerobic growth. *FEBS Lett* 154:343–346.
47. Vink R, Bendall MR, Simpson SJ, Rogers PJ (1984) Estimation of H^+ to adenosine 5′-triphosphate stoichiometry of *Escherichia coli* ATP synthase using ^{31}P NMR. *Biochemistry* 23:3667–3675.
48. Berry S, Rumberg B (1996) H^+/ATP coupling ratio at the unmodulated CF_0F_1-ATP synthase determined by proton flow measurements. *Biochim Biophys Acta* 1276:51–56.
49. Moriyama Y, Iwamoto A, Hanada H, Maeda M, Futai M (1991) One-step purification of *Escherichia coli* H^+-ATPase (F_0F_1) and its reconstitution into liposomes with neurotransmitter transporters. *J Biol Chem* 266:22141–22146.
50. Fischer S, *et al.* (1994) ATP synthesis catalyzed by the ATP synthase of *Escherichia coli* reconstituted into liposomes. *Eur J Biochem* 225:167–172.